Variations in Nuclear Decay Rates

K.-P. Dostal, M. Nagel, and D. Pabst

Zentralinstitut für Isotopen- und Strahlenforschung der Akademie der Wissenschaften der DDR, Leipzig

(Z. Naturforsch. **32 a**, 345–361 [1977]; received January 2, 1977)

This paper is intended to provide a concise introductory review of the fundamental principles underlying the higher-order effects of nuclear decay rate variations which may be produced by physical or chemical means. The first part of the paper embraces the theoretical foundations of the subject matter, and the second deals with methodological and experimental questions. Several tables summarize published experimental results and the pertinent literature.

1. Introduction

This paper aims at providing an introductory review of the fundamental principles underlying the small but measurable variations in nuclear decay rates produced by physical or chemical means. Special emphasis is laid on consistency and conciseness. For this reason the discussion has been restricted to the principal modes of disintegration of alpha, beta, and gamma decay including electron capture and internal conversion for which decay rate changes were predicted by Daudel and Segrè as long ago as 1947.

For ease of reading, the paper has been split into two main parts the first one embracing the theoretical fundamentals, the second dealing with methodological and experimental questions. Several tables have been included in the second part summarizing published experimental results and the pertinent literature.

Earlier reviews of the current subject have been presented by several authors, among them DeBenedetti et al.[1] and Emery[2]. References on work published before 1947 will be found in those articles and have not been replated in our list of references.

2. Theoretical Fundamentals of Nuclear Decay Rate Variations

2.1. General Remarks

The time-dependent Schrödinger equation applied to a perturbed quantummechanical system and solved by Dirac's perturbation method yields in first-order approximation for the transition probability per unit time for a change in the system from the initial state i to one of the accessible final states f[3]

$$W_{\mathrm{fi}} = (2\pi/\hbar)\,|H'_{\mathrm{fi}}|^2 \cdot \varrho(E_{\mathrm{f}}) \qquad (1)$$

Reprint requests to Dr. M. Nagel, Zentralinstitut für Isotopen- und Strahlenforschung der AdW der DDR, Permoserstr. 15, *DDR-705 Leipzig*.

where $\varrho(E_{\mathrm{f}})$ is the energy level density of the final states and H'_{fi} the matrix element of the perturbation H' causing the transition. (1) is known as Fermi's "Golden Rule No. 2". It is this expression which will be the starting point of the present discussion of nuclear decay rate variations. Only alpha decay will be an exception since this case is most conveniently discussed within the framework of Gamov's theory.

In deriving explicit expressions for the decay constant λ, a rigorous treatment must always take into account the influence of the atomic electrons. However, a rough approximation of the type normally found in textbooks on nuclear physics is not sufficient for the present purpose. Variations in the decay rate dealt with in this paper are due to changes in the structure of the atomic electron cloud which may be caused by chemical binding effects etc. Therefore, sufficiently accurate formulae must be derived to enable the evaluation of the magnitude of the small decay rate variations caused by such effects.

2.2. Beta Decay

(1) yields an expression for the beta decay constant of allowed transitions when we assume the parent nucleus to undergo, through the action of a weak perturbation, a transition from the initial state i to the final state f represented by the daughter nucleus, one electron (negatron or positron), and one neutrino. For this purpose, the pertinent interaction matrix element has to be expressed in terms of the normalized eigenfunctions Ψ_{i} and Ψ_{f}:

$$H_{\mathrm{fi}} = \langle \Psi_{\mathrm{f}}^* \,|\, H' \,|\, \Psi_{\mathrm{i}} \rangle \,.$$

The quantity Ψ_{f} can be written as a product of the daughter nucleus wave function ψ_{f} and the lepton wave functions $\varphi_{\mathrm{e}}(r)$ and $\varphi_{\nu}(r)$, the subscripts e and ν referring to the electron and neutrino respectively.

Thus,

$$H_{\mathrm{fi}} = g \,\langle \psi_{\mathrm{f}}^* \,\varphi_{\mathrm{e}}^* (\boldsymbol{r})\, \varphi_{\nu}^* (\boldsymbol{r}) \,|\, M \,|\, \Psi_{\mathrm{i}} \rangle \qquad (2)$$

where g is the Fermi coupling constant and M a Hamilton operator. The lepton wave functions may beforehand be treated as plane waves. Hence,

$$\varphi_j(\boldsymbol{r}) = \tau^{-1/2} \cdot \exp[i(\boldsymbol{k}\cdot\boldsymbol{r})] = \tau^{-1/2} \cdot (1 + i\,\boldsymbol{k}\cdot\boldsymbol{r} + \ldots)$$

where j stands for e and ν, and $\tau^{-1/2}$ is a normalizing factor which proves to be the reciprocal of the spatial volume element under consideration. It can easily be verified that the lepton wavelength $\boldsymbol{\lambda} = k^{-1}$ is in most cases much larger than the nuclear radius. Therefore, it suffices to consider only the first term in the above expansion, i. e., to set $\varphi_j(\boldsymbol{r})$ equal to $\tau^{-1/2}$. This assumption reduces (2) to

$$H'_{fi} = \frac{g}{\tau} \langle \psi_f^* \,|\, M \,|\, \Psi_i \rangle = \frac{g}{\tau} \cdot M_{fi} . \qquad (3)$$

The energy level density factor of (1) is derived by considering the number of possible electron and neutrino states within the spatial volume τ and the momentum interval $[p, p + dp]$ in the 6-dimensional phase space $[x, y, z; p_x, p_y, p_z]$. It can be written as [4]

$$\varrho(E_f) = \frac{\tau^2}{4\pi^4 \hbar^6 c^3} p^2 (E_0 - E)^2 \, dp \qquad (4)$$

where E is the lepton energy (E_0 denotes the maximum of E, i. e. the transition energy). Substituting (4) and (3) into (1) yields the distribution function of the beta momentum spectrum, viz

$$W_{fi} = N(p)\,dp = \frac{g^2}{2\pi^3 \hbar^7 c^3} |M_{fi}|^2 p^2 (E - E_0)^2 \, dp . \qquad (5)$$

The above approximation, treating $\varphi_e(\boldsymbol{r})$ as a plane wave is not quite correct inasmuch as the nuclear Coulomb field distorts the wave function of the emitted electron. This effect is taken into account by introducing, on the right-hand sides of (3) and (5), the Fermi-function $F(Z, E)$ as a correction factor. (The explicit expression for $F(Z, E)$ is a complicated [5] one and need not be discussed here.) If p and E are then expressed in terms of the dimensionless quantity W defined by

$$W = (E + m_0 c^2)/m_0 c^2 \qquad (6)$$

we finally obtain the relationship

$$\lambda_\beta = \int_0^{P \triangleq E_0} N(p)\,dp = \frac{g^2 m_0^5 c^4 |M_{fi}|^2}{2\pi^3 \hbar^7} \cdot \int_1^{W_0} F(Z, W)\,(W^2 - 1)^{1/2} (W_0 - W)^2 W \, dW . \qquad (7)$$

The integral is the well-known Fermi integral function [6].

It is convenient to consider the influence of the atomic electrons at this stage [7]. The atomic electron cloud gives rise to a screening potential V_s lowering the effective Coulomb potential in the vicinity of the nucleus so that the energy of the emitted electron changes from W to

$$W_s = W + V_s \quad \text{or} \quad W_s = W - V_s \qquad (8)$$

for positron and negatron emission respectively. The pertinent correction to (7) can be derived by using a modification of the WKB method [8, 9] which replaces the pure Coulomb Fermi function $F(Z, W)$ by

$$F_s(Z, W) = \frac{(W_s^2 - 1)^{1/2} W_s}{(W^2 - 1) W} F(Z, W_s) . \qquad (9)$$

This yields

$$\lambda_{\beta s} = \text{const} \, |M_{fi}|^2 \int_1^{W_0} F(Z, W_s)\,(W_s^2 - 1)^{1/2} (W_0 - W)^2 W_s \, dW$$

or

$$\lambda_{\beta s} = \text{const.} \, |M_{fi}|^2 f_s . \qquad (10)$$

The quantity f_s will be referred to as the screened Fermi integral function [6].

Altering the structure of the atomic electron cloud of a nuclide, for example by changing the state of valence of an atom, affects the screening potential V_s. As seen from (10), this results in a fractional decay constant variation

$$\frac{\Delta\lambda_\beta}{\lambda_\beta} = \frac{\lambda_{\beta s\,I} - \lambda_{\beta s\,II}}{\lambda_{\beta s\,I}} = \frac{f_{s\,I} - f_{s\,II}}{f_{s\,I}} \qquad (11)$$

with the subscripts I and II denoting the different electron cloud structures.

For light to medium-weight nuclei, the screened Fermi integral function can be rewritten as [10]

$$f_s = f + A(W_0)\, V_s$$

where f is the unscreened integral of (7) and $A(W_0)$ a constant depending only on the endpoint electron energy W_0. Hence,

$$\frac{\Delta\lambda_\beta}{\lambda_\beta} = \frac{\Delta V_s}{V_s} \cdot \frac{f_{s\,I} - f}{f_{s\,I}} . \qquad (12)$$

An appropriate expression for V_s (in electron volts) is [9]

$$V_s \approx 39.45\, Z^{4/3} .$$

The quantity ΔV_s may be assumed to be of the order of 10 eV for all practical cases.

Alder et al.[7] have computed numerical values for $\Delta\lambda_\beta/\lambda_\beta$ as a function of Z and W_0 assuming ΔV_s to be equal to 27.21 eV. The order of magnitude of these values is 10^{-4}. (An exceptional case appears to be tritium where the fractional decay constant

variation may be as great as about 10^{-3} due to the very low transition energy of only 18 keV.) In addition, the graphs presented by Alder et al. show the $\Delta\lambda_\beta/\lambda_\beta$ values to be larger for positron than for negatron emission, and the decay constant variations to become smaller as the transition energy increases. Furthermore, the effect is more pronounced in positron emission for high Z whereas the opposite is true for negatron emission.

Atomic electron screening is usually thought of as playing the most important role in externally induced beta decay rate variations (cf. however p. 169 in [2]). Other atomic effects such as changes in the total atomic binding energy, imperfect atomic wavefunction overlap, electron exchange, and atomic final states distribution, are therefore not discussed in this paper. A concise review of these effects will be found in a recent article by Freedman [11] (see also [12]).

2.3. Electron Capture

The electron capture decay constant λ_{EC} for allowed transitions can be derived from (1) along lines completely similar to those adopted in the treatment of beta decay [3]. However, the energy level density factor depends now only on the neutrino energy $E_{\nu x}$ since the electron is in a definite quantum state x before being captured. It is found to be given by

$$\varrho(E_f) = \tau \cdot E_{\nu x}^2/2\,\pi^2\,c^3\,\hbar^3$$

where the symbols are the same as in 2.2. Furthermore, the electron wave function $\varphi_e(\boldsymbol{r})$ appearing in (2) must be replaced by the wave function $\psi_x(\boldsymbol{r})$ of the orbital from which the electron is captured. It can be supposed to be constant in the vicinity of the nucleus. Thus, according to (1) and (2), the decay constant λ_{ECx} for capture from orbital x can be expressed as

$$\lambda_{ECx} = \text{const}\,|\,\psi_x(0)\,|^2 \cdot E_{\nu x}^2\,, \tag{13}$$

which means that the decay rate is proportional to the electron density at the nucleus. The total decay constant is found by summing up over all orbitals yielding

$$\lambda_{EC} = \sum_x \lambda_{ECx} = \text{const} \sum_x |\psi_x(0)|^2 \cdot (E_0 - E_{Bx})^2 \tag{14}$$

where the neutrino energy $E_{\nu x}$ has been expressed in terms of the transition energy E_0 and the binding energy E_{Bx} of orbital x. The fractional decay constant variation due to the different electron cloud structures I and II can then be written as

$$\frac{\Delta\lambda_{EC}}{\lambda_{EC}} = \frac{\lambda_{EC\,I} - \lambda_{EC\,II}}{\lambda_{EC\,I}} = \frac{\{\sum_x |\psi_x(0)|^2 \cdot (E_0 - E_{Bx})^2\}_I - \{\sum_x |\psi_x(0)|^2 \cdot (E_0 - E_{Bx})^2\}_{II}}{\{\sum_x |\psi_x(0)|^2 \cdot (E_0 - E_{Bx})^2\}_I}\,. \tag{15}$$

The s electrons deliver by far the most important contribution to the electron density at the nucleus [13]. Thus, (15) can be further simplified on assuming the valence shell s electrons to deliver the predominant part to changes in the electron density within the nuclear region [14]. For this outer shell, E_{Bx} is small compared to E_0. The essential term in the denominator of (15) arises from the K shell electrons. The contribution of the other shells can be taken into account by a factor of 1.2. Hence,

$$\frac{\Delta\lambda_{EC}}{\lambda_{EC}} = \frac{E_0^2}{(E_0 - E_{1s})^2} \cdot \frac{\{\sum_i |\psi_i(0)|^2\}_I - \{\sum_i |\psi_i(0)|^2\}_{II}}{1.2\,|\psi_{1s}(0)|^2} \tag{16}$$

where the subscript i refers to the valence shell s electrons only.

Numerical evaluations of the fractional change in the decay constant λ_{EC} based on (15) or (16), can be carried out by means of Hartree-Fock computer programs [15]. The effect increases as Z and E_0 tend to smaller values [16].

It should be borne in mind that (15) and (16) have been derived without considering overlap and exchange effects [17, 18]. This however is justified insofar as such corrections are generally smaller than the accuracy achieved in present-day experiments.

The electron density difference in the numerator of (16) is identical with the difference of the square of the electron wave function at the nucleus which appears as a factor in the formula for the isomer shift in Mössbauer spectroscopy [19, 20]. Therefore, (15) suggests a way of solving the difficult isomer shift calibration problem encountered in Mössbauer work by measuring fractional decay rate changes [21, 22].

2.4. Gamma Ray Emission

The investigation of decay rate variations in gamma ray emission presents a more difficult problem than beta decay and electron capture decay perturbations. The usual method of calculating the decay constant λ_γ consists in applying the "Golden Rule No. 2" of (1) to the single nucleon-electromagnetic field problem without taking into account the existence of the atomic electrons. By making certain simplifications on the nucleon wave functions this approach leads to the formulae of Weiss-

kopf and Moszkowski [23]. It does not of course lend itself to any calculations on how the atomic electrons affect λ_γ.

However, the situation changes if alternatively the retarded interaction between the excited nucleon and the atomic electrons is considered. This is normally done in a semi-classical way and reveals the existence of an additional and competitive decay mode with the decay constant λ_{IC} termed internal conversion and distinguished by radiationless nuclear transitions involving the emission of electrons from the atomic cloud [24]. The decay constant λ_γ still remains unchanged in this approach. If, however, the calculations are based on quantum-field theory as first suggested by Tralli and Goertzel [25], a third-order correction term to λ_γ is found depending on the structure of the electron cloud. Krutov [26] corrected and generalized the results of Tralli and Goertzel and derived solutions of an orbitrarily high order of approximation for the transition probabilities in the shape of recurrence formulae. In the following, the results of Krutov are outlined in brief.

The transition probabilities are calculated employing the time-dependent perturbation theory. The structure of the resulting coupled differential equation system is fixed by assuming an exchange of virtual photons between the nucleon and the electron in question implying certain intermediate states. In accordance with the energy-time uncertainity principle, these states need not conserve energy.

A third-order term expansion of the general solutions given by Krutov [26, 27] yields the following expression for the resulting total decay constant λ if the special case of one K electron and one multipole is considered:

$$\lambda = \lambda^{(1)} + \lambda^{(2)} + \lambda^{(3)} \tag{17}$$

where

$$\lambda^{(1)} = \lambda_\gamma^{(1)} = \frac{2\pi}{\hbar} |H_{K0}|^2 \tag{18}$$

$$\lambda^{(2)} = \lambda_{IC}^{(2)} = \lambda_\gamma^{(1)} \cdot \frac{\pi^2}{(m_0 c^2)^2} |H_{0K}^{eI}|^2 \tag{19}$$

$$\lambda^{(3)} = \lambda_\gamma^{(3)} = \lambda_\gamma^{(1)} \cdot \left[-2\,\Re\mathrm{e}\left\{ \frac{\pi^2}{(m_0 c^2)^2} H_{K0}^{e} H_{0K}^{eI} \right\} + \frac{\pi^4}{(m_0 c^2)^4} |H_{K0}^{e} H_{0K}^{eI}|^2 \right]. \tag{20}$$

The matrix elements are

$$H_{K0} = \sqrt{2\pi k e^2 m_0 c^2}\, \langle \Phi_f | \boldsymbol{\alpha}_n \mathfrak{A}_{LM}^* + U_{LM}^* | \Phi_i \rangle$$

$$H_{K0}^{e} = \sqrt{2\pi k e^2 m_0 c^2}\, \langle \psi_i | \boldsymbol{\alpha}_e \mathfrak{A}_{LM} + U_{LM} | \psi_f \rangle \tag{20 a}$$

$$H_{0K}^{eI} = \sqrt{2\pi k e^2 m_0 c^2}\, \langle \psi_f | \boldsymbol{\alpha}_e \mathfrak{B}_{LM} + V_{LM} | \psi_i \rangle$$

where k is the photon wave number, and $\boldsymbol{\alpha}_e$, $\boldsymbol{\alpha}_n$ are the Dirac vector matrices of the electron and the nucleon respectively. The quantities ψ and Φ are the wave functions of the electron and the nucleus, and $\mathfrak{A}_{LM}$, $\mathfrak{B}_{LM}$, U_{LM}, V_{LM} are the multipole potentials in the denotation used by Rose [28]. (17) to (20) can be generalised to include the case of nuclei surrounded by more than one electron [29, 30] but for the sake of simplicity this problem will not be dealt with in the present paper.

The first-order and second-order terms $\lambda_\gamma^{(1)}$ and $\lambda_{IC}^{(2)}$ are identical with the results of the semiclassical theory. As evident from (18) and (19), the conversion coefficient

$$\beta = \lambda_{IC}^{(2)} / \lambda_\gamma^{(1)} \tag{21}$$

is given by

$$\beta = \frac{\pi^2}{(m_0 c^2)^2} \cdot |H_{0K}^{eI}|^2 . \tag{21 a}$$

The correction terms to $\lambda_\gamma^{(1)}$ appearing in the square brackets on the right-hand side of (20), are most easily interpreted with the aid of Feynman graphs (cf. Figure 1). The positive term is then seen to

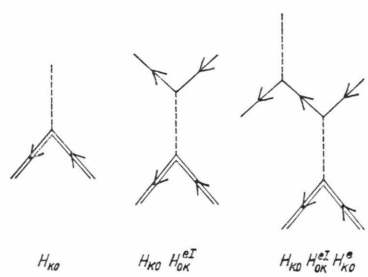

Fig. 1. Feynman graphs of higher-order de-excitation modes. Double lines represent nucleus states, thin lines electron states, and broken lines represent photon states.

describe an additional mode of nucleus deexcitation referred to as the "electronic bridge". In this process, the normal final state of an internal conversion electron represents an intermediate state with the converted electron interacting a second time with the radiation field, losing its kinetic energy by emitting a gamma-quantum, and returning to its discrete state. The negative term in the square brackets of (20) is due to the internal photoeffect and is, in fact, found to be compensated by correspondent positive terms if correction terms of any order higher than three are taken into consideration. – The electronic bridge always outweighs the internal photoeffect for sufficiently large β.

The fractional change of the electronic bridge term in (20) produced by alterations in the struc-

ture of the atomic electron cloud cannot be measured seperately because only changes in the sum value

$$\lambda_\gamma = \lambda_\gamma^{(1)} + \lambda_\gamma^{(3)}$$

can be determined experimentally. Therefore, the fractional decay rate variations in λ_γ must be expected to be smaller than the effects due to internal conversion (cf. 2.5.).

The third-order terms of (20) are calculated on the assumption that energy is conserved in the electronic bridge intermediate state („resonance"). If this assumption, superfluous for the intermediate states, is omitted, additional correction terms („non-resonance terms") arise. We obtain then for the decay constant λ_γ the approximate expression [29, 30]

$$\lambda_\gamma = \lambda_\gamma^{(1)} \cdot \left| 1 - \frac{\pi^2}{(m_0 c^2)^2} H_{K0} H_{0K}^{eI} + \frac{i\pi}{m_0 c^2} \sum_N \frac{\tilde{H}_{K0}^{e} \tilde{H}_{0K}^{eI}}{E_N - E_i - W} \right|^2 \quad (22)$$

where E_i is the initial electron energy level, E_N any discrete intermediate state energy level, and W the nuclear transition energy. In contrast to the quantities used in (20), the matrix elements $\tilde{H}_{K0}^{e}$ and $\tilde{H}_{0K}^{eI}$ are evaluated via two discrete states. The summation in (22) takes into account the fact that now all the unoccupied states of the discrete electron spectrum have to be regarded as intermediate states for the electronic bridge.

The non-resonance correction is of special importance in low energy transitions. One example is the case of the 75 eV transition in U-235m. Here, the ratio of $\lambda_\gamma^{(3)}/\lambda_\gamma^{(1)}$ is found to be 140×10^{-2} if the influence of the whole atomic electron cloud is considered [29].

In general, low energy transitions also feature high conversion coefficients (cf. 2.5.). Therefore highly converted transitions ought to be considered in the first place if chemically or physically induced changes in the decay constant λ_γ are to be investigated. As evident from (20), the fractional decay rate variation measured will be found to be

$$\frac{\Delta\lambda_\gamma}{\lambda_\gamma} = \frac{\Delta(\lambda_\gamma^{(1)} + \lambda_\gamma^{(3)})}{\lambda_\gamma^{(1)} + \lambda_\gamma^{(3)}} = \frac{\left\{\left| 1 - \frac{\pi^2}{(m_0 c^2)^2} H_{K0}^{e} H_{0K}^{eI} \right|^2\right\}_I - \left\{\left| 1 - \frac{\pi^2}{(m_0 c^2)^2} H_{K0}^{e} H_{0K}^{eI} \right|^2\right\}_{II}}{\left\{\left| 1 - \frac{\pi^2}{(m_0 c^2)^2} H_{K0}^{e} H_{0K}^{eI} \right|^2\right\}_I}$$

for the resonance case, with the Roman subscripts again denoting the two different electron shell structures under consideration. For highly converted transitions,

$$\left| 2\,\mathfrak{Re}\left\{ \frac{\pi^2}{(m_0 c^2)^2} H_{K0}^{e} H_{0K}^{eI} \right\} \right| \ll \frac{\pi^4}{(m_0 c^2)^4} \left| H_{K0}^{e} H_{0K}^{eI} \right|^2$$

and

$$1 \gg \frac{\pi^4}{(m_0 c^2)^4} \left| H_{K0}^{e} H_{0K}^{eI} \right|^2$$

whence

$$\frac{\Delta\lambda_\gamma}{\lambda_\gamma} = \frac{\pi^4}{(m_0 c^2)^4} \cdot \left[\left\{ \left| H_{K0}^{e} H_{0K}^{eI} \right|^2 \right\}_I - \left\{ \left| H_{K0}^{e} H_{0K}^{eI} \right|^2 \right\}_{II} \right]. \quad (23)$$

The theoretical computation will be facilitated by the fact that the electron matrix elements appearing in (23), can generally be reduced to radial integrals and numerically evaluated [26, 27, 29]. To the authors' knowledge, however, no relevant theoretical or experimental results have been reported up to the present date.

2.5. *Internal Conversion*

The conversion coefficient β defined by (21) relates to a relativistic electron making a transition from the initial state of quantum number $\varkappa'$ to the final state of quantum number $\varkappa$. Considering (20 a), the relationship (21 a) can therefore be rewritten as

$$\beta_{\varkappa'} = 2\pi^3 \frac{e^2}{\hbar c} \cdot \frac{W}{m_0 c^2} \sum \left| \langle \psi_\varkappa | \boldsymbol{\alpha}_e \mathfrak{B}_{LM} + V_{LM} | \psi_{\varkappa'} \rangle \right|^2. \quad (24)$$

In this expression, we have to average over M and to sum up over all possible final states $\varkappa$, their projection quantum numbers μ, and the initial state projection quantum numbers μ' [28].

Calculating the total decay rate of internal conversion requires summation over the quantum numbers $\varkappa'$ of all the single shells. As apparent from (21), this yields

$$\lambda_{IC} = \lambda_\gamma \cdot \sum_{\varkappa'} \beta_{\varkappa'} \quad (25)$$

where now λ_{IC} and λ_γ refer to the quantities obtained in the usual approximation.

Alterations of the electron cloud caused externally result in changes of the partial conversion coefficients as evident from (24). Hence, if λ_γ is assumed to be constant, we obtain

$$\frac{\Delta\lambda_{IC}}{\lambda_{IC}} = \frac{1}{\beta} \sum_{\varkappa'} \Delta\beta_{\varkappa'} = \frac{1}{\beta} \sum_{\varkappa'} \beta_{\varkappa'} \frac{\Delta\beta_{\varkappa'}}{\beta_{\varkappa'}}. \quad (26)$$

If conversion in the inner shells is forbidden for energetical reasons, the outer shells always exhibit large partial conversion coefficients. As seen from (26) this means that the relative changes $\Delta\beta_{\varkappa'}/\beta_{\varkappa'}$ are multiplied by large weight factors. For this reason, appreciable values of $\Delta\lambda_{IC}/\lambda_{IC}$ are to be expected with low excitation energy transitions (which are always strongly converted). (26) also indicates the possibility of determining $\Delta\lambda_{IC}/\lambda_{IC}$ by measuring selectively the relative changes of the partial conversion coefficients with the aid of a beta spectrometer [31–35].

The wave function $\psi_{\varkappa'}$ in (24) is multiplied by the Hankel function included in the interaction operator. This function drops to a value near zero outside the K shell region and hence allows the integration to be restricted to the region inside the K shell [36]. Therefore the relationship

$$\beta_{\varkappa'} \propto |\psi_{\varkappa'}(0)|^2$$

is a reasonably good approximation and (26) can be written [37]

$$\frac{\Delta\lambda_{IC}}{\lambda_{IC}} = \frac{1}{\beta}\sum_{\varkappa'}\beta_{\varkappa'}\,\frac{\Delta|\psi_{\varkappa'}(0)|^2}{|\psi_{\varkappa'}(0)|^2}. \qquad (26\,a)$$

In the special case of M1 transitions, which are mainly converted in s shells [38], (26 a) can be further reduced to the simple formula

$$\frac{\Delta\lambda_{IC}}{\lambda_{IC}} = \frac{\Delta|\psi(0)|^2}{|\psi(0)|^2} \qquad (27)$$

where only those s shells contribute to $|\Psi(0)|^2$ which take part in the conversion.

(27) suggests that is also possible to solve the isomer shift calibration problem of Mössbauer spectroscopy already mentioned in 2.3., by measuring fractional decay rate changes of conversion transitions [38–41].

The order of magnitude to be expected for $\Delta\lambda_{IC}/\lambda_{IC}$, can be assessed by evaluating, for different free-ion electron configurations, the quantities on the right-hand side of (26) and (27) [38, 42]. In such calculations, we must take into account not only the valence electron changes but also the rearrangement of the whole atomic core caused by screening effects [43]. The accuracy required is assured if the conversion coefficients and the electron densities at the nucleus are calculated by using relativistic Hartree-Fock programs [38, 44].

2.6. *Alpha Decay*

According to Gamov's theory of alpha decay, the decay constant λ_α can be written as a product of two factors, one representing the repetition rate λ_0 of an alpha particle running against the inner side of the surrounding nuclear potential barrier, the other constituting the probability P of the alpha particle penetrating through that barrier [4]:

$$\lambda_\alpha = \lambda_0 \cdot P\,. \qquad (28)$$

Since λ_0 may be supposed to depend entirely on nuclear properties, only the transmission coefficient P need to be dealt with for the present purpose. It is given by the expression

$$P = \exp\left\{-\frac{2\sqrt{2m}}{\hbar}\int_R^{r_t}\sqrt{V(r)-E_0}\,dr\right\} \qquad (29)$$

where m is the reduced mass of the alpha particle, E_0 the transition energy, R the nuclear radius, and r_t the outer classical turning point. $V(r)$ stands for the radially symmetric Coulomb potential of the daughter nucleus. For nonzero angular momentum of the alpha particle, a centrifugal potential V_l has to be added to $V(r)$. This however, may be neglected in the following.

Benoist-Gueutal was the first to point out that a rigorous treatment of alpha decay must take into account the effect of the atomic electrons [47, 48]. According to Erma [49], this can be done by substituting the nuclear Coulomb potential $V(r)$ in (29) by

$$U(r) = V(r) - 2V_s(r) = \frac{2(Z-2)}{r} - 2V_s(r)$$

where $V_s(r)$ is the screening potential of the atomic electrons (cf. 2.2.). The fractional decay rate variation due to changes of $V_s(r)$ can then be calculated by taking the logarithm on both sides of (29) and differentiating:

$$\frac{\Delta\lambda_\alpha}{\lambda_\alpha} = \frac{P_I - P_{II}}{P_I} \qquad (30)$$

$$= \delta \ln P = \sqrt{2m}\int_R^{r_t}\frac{\delta[V(r)-2V_s(r)-E_0]}{\sqrt{V(r)-2V_s(r)-E_0}}\,dr\,.$$

The screening potential $V_s(r)$ is constant within the range $0 \leqq r \leqq R$ (cf., [50]). This means that any variation of $V_s(r)$ in this region results not only in a change of the transition energy E_0 but leads also to a change (of the same magnitude and sign) in the height of the potential barrier surrounding the alpha particle. Therefore, the only alteration in the decay constant which may be caused by affecting the electron cloud structure, must be due to the de-

pendence of $V_s(r)$ on r and the electron density in the range $R \leqq r \leqq r_t$:

$$\delta[V(r) - 2V_s(r) - E_0] = -2\delta V_s(r) \equiv -2\Delta V_s(r) .$$

The quantity $V_s(r)$ can be computed by assuming the nucleus to be surrounded by a spherical shell of constant electron density $|\psi(0)|^2$ the shell being bounded by the nucleus of radius R and a sphere of radius r_t [51]. The electrostatic potential within this spherical shell is

$$V_s(r) = V_s(R) - 2\pi|\psi(0)|^2 R^2 + \frac{2\pi}{3}|\psi(0)|^2 r^2\left(1 + \frac{2R^3}{r^3}\right).$$

The terms in R^2 and R^3 may be neglected. Hence,

$$2\Delta V_s(r) = \frac{4\pi}{3} r^2 \Delta|\psi(0)|^2$$

and

$$\frac{\Delta\lambda_\alpha}{\lambda_\alpha} = \sqrt{2m}\,\frac{4\pi}{3}\Delta|\psi(0)|^2 \int_R^{r_t} \frac{r^2\,dr}{\sqrt{\frac{2(Z-2)}{r} - E_0 - 2V_s(R) - \frac{4\pi}{3}|\psi(0)|^2 r^2}} . \quad (31)$$

(31) can be further simplified taking into account that

$$R \approx 0, \quad V_s(R) \ll E_0, \quad (4\pi/3)|\psi(0)|^2 r^2 \ll E_0 .$$

The final relationship thus obtained is [51]

$$\Delta\lambda_\alpha/\lambda_\alpha \approx 4000\,(Z-2)^3\,E_0^{-7/2}\,\Delta|\psi(0)|^2 \quad (32)$$

where E_0 and $\Delta|\psi(0)|^2$ are in atomic units. The maximum error of this approximation as compared to (31), amounts to only 5 per cent.

According to (31), the removal of one 6s electron causes a fractional decay constant variation of about 7×10^{-8} in Sm-147 [51]. A similar estimate for the case of Ra-226 led to a fractional change of 1.7×10^{-7} assuming one 7s electron to be removed [2]. Larger values reported by other authors [52] appear to be incorrect, the calculations being based on an erroneous model.

3. Methodology and Experimental Results

3.1. Methods of Measuring Decay Rate Variations

The subject matter of this Section can be subdivided into two parts, the first one dealing with methods for altering the electron cloud structure of the atoms under consideration, the second discussing the various procedures employed in detecting the resulting decay constant changes.

The most obvious way of bringing about a drastic alteration in the electron cloud structure is to ionize the atom as far as possible by extra-atomic means. Such experiments have been proposed by several authors [53–55]. However, the technical difficulties involved appear to be formidable. Apart from some work on internal conversion in recoil ions from alpha decay [56] and Coulomb excited nuclei [57], no successful experiments of this kind have been reported up to the present date.

A much easier, and in point of fact, the most widely used, approach is to investigate how the decay rate is influenced by chemical binding effects. This can be done by measuring the decay constant difference of samples in which the atoms are in different valence states. The experimental results must then be interpreted in a way similar to the well-known discussion of isomer shifts in Mössbauer spectroscopy [20, 35, 37, 42].

An external electric field may cause a change in the electron density at the nucleus of an atom occupying a lattice site of a dielectric solid. In certain cases, this change will be proportional to the strength of the applied field [58]. This effect has been employed to produce fractional decay constant variations of the order of some 10^{-5} by applying a field of about 10^4 V/cm to Tc-99m samples [59]. – The influence of internal electric fields on the decay rate has also been studied for several cases [60–62].

External magnetic fields are not likely to produce any decay constant variation. The theoretical treatment of the Zeeman effect reveals [63] that the radial part of the electron wave functions is not affected by a magnetic field. For this reason, the electron density at the nucleus which in general plays the essential role in decay rate variations, likewise remains unchanged.

Pressure squeezes the electron wave functions of the valence electrons, which normally results in an increase in the electron density in the vicinity of the nucleus [64–67]. However, the amount of energy transferred to each atom of the sample through the compression is hardly greater than that taken up by the sample atoms in a chemical reaction. This is true at least as long as pressure values are considered which are achievable under laboratory conditions (about 500 kbar). Therefore, if the energy transferred is regarded as a qualitative measure of the correspondent alteration of the electron cloud structure, the

resulting decay rate variation must be expected not to exceed the magnitude of the effect obtainable by chemical means.

The direct transfer of electrons from one band to another [68] which occurs in some metals already at relatively low pressure values (for example in the case of caesium at about 44 kbar) has not yet been employed in decay rate variation experiments.

The superconductivity transition temperatures of technetium (11.2 °K) and niobium (9.2 °K) are comparatively high. This suggests investigations on how internal conversion in Tc-99m and Nb-90m is affected by superconductivity. Such experiments have been carried out by Byers et al.[69], Cooper [70] and Olin et al.[71]. The results were positive (cf. 4). The magnitude of the effects observed is however not well understood.

A summary of the methods applicable to the detection of decay rate variations, is given in Table 1. For lack of space, only short explanatory comments can be presented here. Details will be found in the references cited.

The half-life ranges listed in Table 1, should be regarded as very rough estimates only. Nonetheless, the values reveal that obviously no method has been developed so far which could be employed for detecting decay constant variations in nuclides having half-lives in the range from about one microsecond to several tens of seconds. This is in contrast to the fact that there *are* some nuclides within this range which appear to be promising for experimental work [45, 46].

The delayed coincidence technique is a standard method and need not be discussed any further in this context. A few words on the other methods, however, seem to be appropriate.

The applicability of the perturbed equilibrium method requires the existence of a suitable parent-daughter decay scheme. If the daughter, supposed to have a short life-time in comparison to its parent, is in equilibrium with the parent, a sudden change in the daughter decay constant from λ_D to $\lambda_D + \Delta\lambda_D$, for example due to a rapid chemical reaction will perturb the equilibrium and cause a change in the daughter activity A. The equilibrium will then be restored with the half-life of the daughter in its altered chemical environment. A formula for the change with time of the daughter activity can be derived by solving the general differential equation for a series decay scheme (cf. [78]). For the simplest case (no competing decay modes in the disintegration scheme of parent or daughter, and detection of only the daughter activity), the relationship desired is found to be

$$\frac{A_a(t) - A_b}{A_b} = \frac{\lambda_D + \Delta\lambda_D}{\lambda_D} \cdot e^{-(\lambda_D + \Delta\lambda_D)t} - e^{-\lambda_D t}$$

where the subscripts b and a refer to time before and after the reaction. Thus, A_b is a constant. The reaction is supposed to have taken place at $t = 0$. It is evident that $\Delta\lambda_D$ can be determined from the steplike change in the daughter activity which occurs at $t = 0$.

The Rutherford differential method is based upon measuring the difference in the output currents of two suitable detectors put up in front of two samples, the decay constants of which are assumed to differ by $\Delta\lambda$. The current difference at time t is given by

$$I_1(t) - I_2(t) = I_1(0)\, e^{-\lambda t} - I_2(0)\, e^{-(\lambda + \Delta\lambda)t}\,.$$

For small $\Delta\lambda \cdot t_1$

$$I_2(t) \approx I_2(0)\, e^{-\lambda t}\,(1 - \Delta\lambda\, t)\,.$$

Table 1. Methods of detecting decay rate variations.

Method	Appropriate half-life range	Comment	Example of application	References
Delayed coincidence technique	10 ns $\leqq T_{1/2} \leqq$ 1 μs	Half-lifes of different samples directly measured.	Fe-57 m	72, 39
Perturbation of radioactive equilibrium	20 s $\leqq T_{1/2} \leqq$ 1 h	Variation with time of activity measured, following a rapid change in decay constant due to chemical reaction, alteration of pressure, or change of temperature.	Nb-90 m	73
Rutherford differential method	30 min $\leqq T_{1/2} \leqq$ 100 d	Change with time of activity difference of two samples measured.	Tc-99 m	74, 61
Quasi-differential approach	30 min $\leqq T_{1/2} \leqq$ 100 d	Change with time of ratio of counting rates, i. e. activities, of two samples measured.	Zr-89	60, 62
Mass-spectroscopic measurements	2 d $\leqq T_{1/2} \leqq$ 10 y	Change with time of isotope abundance ratio of two samples determined.	H-3	76
Decay curve measurements	10 min $\leqq T_{1/2} \leqq$ 100 d	Half-lives of different samples directly measured.	U-235 m	77

Hence,

$$\{I_1(t) - I_2(t)\}\, e^{\lambda t} = I_1(0) - I_2(0) + I_2(0)\,\Delta\lambda\, t\,.$$

Thus the decay constant difference $\Delta\lambda$ is easily obtained from a least-square fit of the measured values to this function.

The differential method is very sensitive and reliable since errors due to gain drifts etc. are largely cancelled out.

Similar advantages are offered by the quasi-differential approach first described by Huber et al.[79]. It consists essentially in placing, in turns, two samples in front of a detector, and determining the change with time of the ratio $Q(t)$ of the counting rates. Since these are proportional to the activities of the samples, $Q(t)$ may be written as

$$Q(t) = \frac{(\lambda + \Delta\lambda)\, N_{01}\, e^{-(\lambda+\Delta\lambda)t}\, \Delta t}{\lambda\, N_{02}\, e^{-\lambda(t+\Delta t+\delta t)}\, \Delta t}$$

where Δt is the measuring interval, δt the time elapsing during the interchange of the samples, and N_{01}, N_{02} the initial numbers of the respective nuclei. Considering that $\Delta\lambda\, t \ll 1$, this equation can be reduced to

$$Q(t) = (1 + \Delta\lambda/\lambda)\, \frac{N_{01}}{N_{02}}\, e^{\lambda(\Delta t+\delta t)}\, (1 - \Delta\lambda\, t)\,.$$

The ansatz for $Q(t)$ shows that the fractional decay constant variation $\Delta\lambda/\lambda$ can be determined via $Q(t)$ in two ways. If $\Delta\lambda$ is kept constant for the whole time of the experiment, $Q(t)$ varies linearly with time the slope of the resulting curve yielding $\Delta\lambda$ ("slope method"). Alternatively, the influence producing $\Delta\lambda$, may be periodically switched on and off leading to steplike changes in $Q(t)$ with the height of the steps giving $\Delta\lambda$ ("step method"). Both methods have been successfully employed.

The quasi-differential approach has been used to measure decay rate variations as small as $(4.9 \pm 2.9) \times 10^{-5}$ [80].

The mass-spectroscopic method[76] can be employed only if the decay mode under consideration involves a change in the nuclear charge Z. It takes advantage of the fact that the isotopic abundance ratios in two (or more) compounds prepared from a given isotope mixture, will be found to differ by a small amount after some time if the decay constant is not the same in the various samples. The beta decay of tritium may serve as an illustrative example. The abundance ratios of two samples made from a protium-tritium mixture, can be expressed as

$$N_T\, e^{-\lambda t}/N_P$$

and

$$N_T\, e^{-(\lambda+\Delta\lambda)t}/N_P$$

Thus, the fractional abundance ratio difference (the δ value) may be written as

$$\delta(t) = \frac{N_T\, e^{-\lambda t}/N_P - N_T\, e^{-(\lambda+\Delta\lambda)t}/N_P}{N_T\, e^{-\lambda t}/N_P}$$

whence

$$\delta(t) = 1 - e^{-\Delta\lambda t} \approx \Delta\lambda\, t\,.$$

In the case of a protium-tritium mixture, δ values of the order of some 10^{-4} can be measured with sufficient accuracy. Hence, it will be some years after preparing the samples, that the fractional decay constant variation of about 10^{-3} as predicted by Alder et al.[7] becomes detectable. This outcome leads to the conclusion that the mass-spectroscopic method may prove to be of special advantage in experiments involving long-lived nuclides. The determination of decay constant variations by directly measuring the decay curve requires an accuracy not normally achievable (see however [81, 82]). An exception is the case of U-325m where fractional half-life changes of the order of some 10^{-2} have been found using this method[77].

3. 2. Experimental Results

All experimental results on physically or chemically induced decay rate variations published since 1947 and known to the authors are summarized in Tables 2, 3 and 4, the nuclides being arranged according to atomic number. For the sake of completeness, even questionable and negative results have been listed. The nuclides Cu-64 and Ag-108 both of which decay via negatron and positron emission as well as electron capture are to be found in Table 2. With one exception[83], no newer experiments have been reported on alpha and positron decay or gamma ray emission up to the present date.

Unless otherwise indicated, the decay constant variation $\Delta\lambda$ is meant to be the difference $\lambda_1 - \lambda_2$ with λ_1 denoting the first and λ_2 the second sample given in Column 4 *. Some important results of essential experiments aimed at investigating chemical and physical effects on partial internal conversion coefficients have been included in Table 4.

4. Conclusions

The work on nuclear decay rate variations may now be regarded as an established field of fruitful research. Not only does it furnish valuable information on higher-order processes in nuclear decay but it also helps to solve the difficult isomer shift calibration problem of Mössbauer spectroscopy and,

* Some values are calculated from the original values by the authors.

Table 2. Electron capture experiments.

Z	Nuclide	$T_{1/2}$	Source Combination	$\frac{\lambda}{\Delta\lambda} \times 10^3$	Ref.	Comment
1	2	3	4	5	6	7
4	Be-7	53.5 d	Be $-$BeO	0.15 ± 0.09	84	First suggestions
			Be $-$BeO	0.131 ± 0.05	85	in [91, 92]; preliminary
			BeO$-$$BeF_2$ (hexagonal form)	0.69 ± 0.03	86	results in [93–98].
			BeO$-$$BeF_2$ (hexagonal form)	0.609 ± 0.055	85	For interpretation
			BeO$-$$BeF_2$ (amorphous form)	1.130 ± 0.058	87	of these results,
			Be $-$$BeF_2$ (hexagonal form)	0.741 ± 0.047	85	see [47, 48, 87, 95, 97, 99]
			Be $-$$BeF_2$ (amorphous form)	1.2 ± 0.1	88	Establishment of
			BeS $-$Be	0.53 ± 0.06	89	scale for relative
			BeO$-$$BeBr_2$	1.472 ± 0.063	87	electron densities
			BeO$-$$Be(C_5H_5)_2$	0.795 ± 0.074	87	at nucleus in
			$Be^{2+}(OH_2)_4$$-$BeO	0.374 ± 0.077	87	various compounds,
			$Be_4O(CH_3COO)_6$$-$BeO	0.724 ± 0.057	87	understanding of
			$Be^{2+}(OH_2)_4$$-$$Be(C_5H_5)_2$	1.169 ± 0.106	87	real chemical bond
			$Be_4O(CH_3COO)_6$$-$$BeF_2$ (amorphous form)	1.852 ± 0.082	87	structures, open
			$^7BeCO_3 \cdot Be(OH_2)$ at normal pressure, at 140 kbar, and 157 kbar.	(2 ± 3)/100 kbar	90	questions as to effects of bond lengths and electronegativity of binding partners.
			BeO at normal pressure, at 120 kbar, at 210 kbar, and at 270 kbar.	(2.2 ± 0.1)/ 100 kbar		Magnitude of effect consistent with theoretical estimates [66]. Cf. also [67]
			$Be_2P_2O_7$$-$$Be(OH_2)_4$	1.803 ± 0.43	151	
29	Cu-64	12.8 h	Dissolved copper salt compared to metal: $[CuSO_4]_{soln}-Cu_{metal}$	17.0 ± 6.4	100	Effects reported surprisingly large. See also [102].
			$[Cu(NH_3)_4SO_4]_{soln}-Cu_{metal}$	-8.7 ± 3.0	100	
			Annealed α copper phthalocyanine sample compared to unannealed sample both containing thermal neutron generated ^{64}Cu.	1.0 ± 0.16	101	
			Cu$-$CuO	0.0 ± 0.3	75	
			Cu$-$$Cu(NO_3)_2$ (liquid)	0	152	
			Annealed β copper phtalocyanine compared to irradiated sample	0.043 ± 0.2	153	
			Cu$-$$Cu(H_2O)_6SO_4$	0.112 ± 0.009	154	
			Cu$-$$Cu(H_2O)_4(NO_3)_2$	0.081 ± 0.01		
			β CuPc (h) $-$ β CuPc (irr)	0.14 ± 0.23	155	Pc = phtalocyanine
			α CuPc (h) $-$ α CuPc (irr)	0.37 ± 0.58		h = annealed,
			Cu (metal) $-$CuO	0 ± 0.23		irr = irradiated
38	Sr-85	65.2 d	Strontium replacing barium in ferroelectric and paraelectric $BaTiO_3$ single crystals.	0.049 ± 0.029	80	
40	Zr-89	78.4 h	Zirconium replacing titanium in paraelectric and ferroelectric $BaTiO_3$ single crystals.	0.62 ± 0.02	60	Effect attributed solely to electron capture resulting in $\Delta\lambda_{EC}/\lambda_{EC} = (0.8 \pm 0.03) \times 10^{-3}$. Cf. [103].
			As above.	0.44 ± 0.04	79	Apparently, not all zirconium atoms integrated into $BaTiO_3$ lattice. Cf. [60].
			As above.	0.62 ± 0.24	62	
			Antiferroelectric $PbZrO_3$ sample	1.32 ± 0.08	62	
			compared to paraelectric sample.	1.24 ± 0.04		
			$PbZrO_3$ sample at 200 °C compare to	0.11 ± 0.16	62	Proof of zero temperature effect on ^{89}Zr decay rate in antiferroelectric $PbZrO_3$ phase.
			sample at 30 °C.	0.10 ± 0.8		

Table 2, continued.

Z	Nuclide	$T_{1/2}$	Source combination	$\frac{\Delta\lambda}{\lambda} \times 10^3$	Ref.	Comment
1	2	3	4	5	6	7
			Monoclinic ZrO_2 sample at 30 °C compared to monoclinic sample at 350 °C.	$\begin{cases} 0.63 \pm 0.06 \\ 0.42 \pm 0.11 \end{cases}$	62	
			Monoclinic ZrO_2 sample at 30 °C compared to cubic sample at 30 °C.	0.07 ± 0.05	62	
44	Ru-97	2.9 d	$[Ru^{III}(NH_3)_5Cl]Cl_2 - Ru_{metal}$	-0.116 ± 0.025	21	Theoretical interpretation given.
			$Ru_{0.03}Pt_{0.97}$ (alloy) $- Ru_{metal}$	-0.104 ± 0.027	21	Results used to determine mean-square radius differences between excited and ground states of Mössbauer nuclei Ru-99 (89 keV) and Ru-101 (127 keV).
			$KRuO_4 - Ru_{metal}$	0.263 ± 0.024	21	
47	Ag-108	2.4 min	$Ag_{metal} = AgNO_3$	13 ± 10	82	Effect surprisingly large.
53	J-125	60 d	—		104	Results not yet published.
56	Ba-131	12 d	Sample at 100 kbar compared to sample at normal pressure.	0.66	90	

Table 3. Negatron decay experiments.

Z	Nuclide	$T_{1/2}$	Source combination	$\frac{\Delta\lambda}{\lambda} \times 10^3$	Ref.	Comment
1	2	3	4	5	6	7
1	T	12.3 a	—	—	76 7	Experimental work planned Alder's theory predicts $\Delta\lambda/\lambda \approx 10^{-3}$ [7]. Cf. [113, 114].
11	Na-24	15 h	Water-dissolved NaCl sample compared to solid sample.	5.2 ± 2.0	105	Results doubted by some authors [7, 115, 116].
			Same as above.	<1	106	In agreement with Alder's theory.
			$Na_2CO_3 - Na$ (liquid)	0	152	
			Na (metal) $- NaNO_3$	-8.5 ± 3.6	156	
13	Al-28	2.3 min	Metal sample compared to oxide sample.	0	82	
23	V-52	3.77 min	Metal sample compared to V_2O_5 and to vanadium oxisulfate.	0	82	
27	Co-60	5.26 a		—	107	No details published.
53	J-131	8.1 d	Solid NaJ sample compared to water-dissolved NaJ.	>0	107	Results doubted by some authors [110].
			As above.	43 ± 21	108	Results doubted by some authors [7, 110].
			As above.	26.4 ± 23	—	Work referred to in [117].
			As above	0	109	
			Solid NaJ sample compared to liquid J^- and AgJ precipitate samples.	0	110	
			Measurement of $T_{1/2}$ of some Iodine compounds		152	
			NaI (solid) $-$ NaI (liquid)	0.07 ± 0.15	158	
			NaI (solid) $- NaIO_3$ (solid)	0.14 ± 0.14		
58	Ce-144	284 d	—	—	107	No details published.
79	Au-198	2.7 d	$Au_{metal} - Au_2O_3$	0.1 ± 0.03	111 112	In agreement with Alder's theory [7].
			$Au_{colloid} - Au_{solid}$	7.3 ± 6.7	157	

Table 4. Internal conversion experiments.

Z	Nuclide	E_0 $T_{1/2}$	Source combination	$\frac{\Delta\lambda}{\lambda}\times 10^3$	Ref.	Comment
1	2	3	4	5	6	7
21	Sc-46m	142 keV	Metallic sample compared to oxide sample.	0	82	Cf. [81, 120].
26	Fe-57m	14.4 keV 98.5 ns	Pt(^{57}Fe) sample compared to Pt(^{57}Fe; HCl), Pt(^{57}Fe, HCl, annealed), and Fe(^{57}Fe) sample.	—	34	Conversion ratios measured. Results: $\alpha_{4s}/\alpha_{3s}=3.8\times10^{-2}$ for Pt(^{57}Fe) samples, and $\alpha_{4s}/\alpha_{3s}=6.6\times10^{-2}$ for Fe(^{57}Fe) sample. For discussion, cf. [38].
			Metallic state source compared to oxide state source.	—	118	Conversion ratios measured. Results: $\alpha_{4s}/\alpha_{3s}=3.4\times10^{-2}$ for "metallic" state source, and $\alpha_{4s}/\alpha_{3s}=2.4\times10^{-2}$ for "oxide" state source. Cf. [121].
			Annealed and unannealed sources compared. Sources prepared by diffusing ^{57}Co into Co metal.	—	119	Conversion spectra found to be different for the two sources: $\alpha_{4s}/\alpha_{3s}=2.84\times10^{-2}$ for unannealed source, and $\alpha_{4s}/\alpha_{3s}=3.45\times10^{-2}$ for annealed source.
			^{57}Fe in matrices of:			
			CoO and Co	-0.63 ± 0.13	122	First experiments to solve the isomer shift calibration problem in Mössbauer spectroscopy by measuring decay rate variations.
			CoO and Cu	-0.48 ± 0.14	123	
			Au and Co	-0.44 ± 0.14	72	
			CoO and Au	-0.22 ± 0.15	39	
			Au and Cu	-0.34 ± 0.15		
			Cu and Co.	-0.17 ± 0.14		
			^{57}Fe in matrices of zinc and vanadium.	0.42 ± 0.22	40	
34	Se-77m	161 keV 17.9 s	$Se_{metal}-SeO_4Na_2$	8.3 ± 5.6	82	Effect surprisingly large.
			$Se_{metal}-KSeCN$	10.6 ± 5.0	82	Effect surprisingly large.
41	Nb-90m	2.4 keV 19 s	Metallic state compared to fluoride complex state.	36 ± 4	73 70	
			Metallic state compared to superconducting sample.	0	70	Effect shown to be smaller than 2×10^{-3}.
			Sample at pressure of 0.1 megabar compared to sample at normal pressure.	0	70	
			Metallic state compared to fluoride complex state.	0	124	Effect shown to be smaller than 10×10^{-3}.
			Normal sample compared to superconducting sample.	1.95 ± 0.55	71	
			Metallic state compared to fluoride complex state.	39 ± 8	125	
			Nb_2O_5 sample compared to metal sample.	18.7 ± 5	125	
			Nb atoms in Zr metal compared to fluoride complex sample.	0	42	Effect shown to be smaller than 1.8×10^{-3}. Results of other authors discussed and interpretation given.
			Nb in Zr compared to Nb in Hf	0	159	
43	Tc-99m	21.17 keV 6.0 h	$KTcO_4-Tc_2S_7$	2.70 ± 0.10	126 74	
			$Tc_{metal}-Tc_2S_7$	0.31 ± 0.12	126	
			$NaTcO_4-Na_2TcCl_6$	2.7 ± 0.4	74	Authors' results. Details to be published elsewhere.
			Sample at pressure of 0.1 megabar compared to sample at normal presure.	0.23 ± 0.05	127	Results consistent with theoretical estimate [64].

Table 4, continued.

Z	Nuclide	E_0 $T_{1/2}$	Source combination	$\frac{\Delta\lambda}{\lambda}\times 10^3$	Ref.	Comment
1	2	3	4	5	6	7
			Sample at 77 K compared to sample at 293 K.	0	69	
			Superconducting sample at 4.2 K compared to normal sample at 293 K.	0.64 ± 0.04	69	
			Normal sample at 4.2 K compared to sample at 293 K.	0.13 ± 0.04	69	
			Normal sample compared to sample exposed to electric field, at normalized field strength of		128 59 129	
			10^4 V/cm: K_2TcJ	0.0305 ± 0.0045		
			K_2TcBr	0.0260 ± 0.0035		
			K_2TcCl_6	0.0295 ± 0.0040		
			K_2TcF_6	0.0110 ± 0.0045		
			$KTcO_4$	0.0145 ± 0.055		
			$NaTcO_4$	$0.163\ \pm0.026$		Samples containing sodium
			Na_2TcCl_6	$0.06\ \pm0.01$		said to have been carrier-free.
			Technetium replacing titanium in paraelectric and ferroelectric $BaTiO_3$ samples.	$2.6\ \pm0.4$	61	
			Sample at pressure of 0.1 megabar compared to sample at normal pressure	$0.46\ \pm0.23$	65	In agreement with Bainbridge's results. Cf. [131].
			Sample exposed to strong centrifugal field, compared to normal sample.	—	130	No details published. Experimental results lacking.
50	Sn-119m	23.9 keV 17.8 ns	SnO_2 samples compared to white tin samples.	—	31	First conversion ratio measurements used to solve isomer shift calibration problem in Mössbauer spectroscopy. Results: $\alpha_{5s}/\alpha_{4s}=(7.4\pm0.4)\times10^{-2}$ for SnO_2 and $\alpha_{5s}/\alpha_{4s}=(10.8\pm0.3)\times10^{-2}$ for white tin. Cf. [38, 132, 133].
			$Sn(SO_4)_2-SnS_2$	-0.34 ± 0.24	104,	Decay rate variation measured
			$Sn(SO_4)_2-\beta$ tin	-0.82 ± 0.30	41	to solve isomer shift calibration problem for Sn-119m.
			$Sn(SO_4)_2-SnCl_2$	-1.35 ± 0.26		Values calculated from Fig. 4
			$Sn(SO_4)_2-SnJ_4$	-0.42 ± 0.31		in [41].
			$Sn(SO_4)_2-SnS$	-1.19 ± 0.28		
52	Te-125m$_1$	109 keV 58 d	$Te_{elemental}-Ag_2Te$	0.259 ± 0.018	134	
			$TeO_2\quad -Ag_2Te$	0.223 ± 0.018		
			$Te_{elemental}-TeO_2$	0.036 ± 0.017		
	Te-125m$_2$	35.6 keV 1.5 ns	$Te_{metal}\quad -ZnTe$	—	33	Conversion ratios measured. Results: $\alpha_{5s}/\alpha_{4s}=(15.2\pm1.7)\times10^{-2}$ for metallic Te and $\alpha_{5s}/\alpha_{4s}=(10.8\pm1.5)\times10^{-2}$ for ZnTe.
			$TeO_2\quad -ZnTe$	—	35	Conversion ratios measured.
			$TeO_2\quad -Na_2H_4TeO_6$	—		Results: $\alpha_{5s}/\alpha_{4s}=(13.0\pm0.9)\times10^{-2}$ for TeO_2, $\alpha_{5s}/\alpha_{4s}=(11.7\pm0.7)\times10^{-2}$ for ZnTe, $\alpha_{5s}/\alpha_{4s}=(5.1\pm1.5)\times10^{-2}$ for $Na_2H_4TeO_6$. Cf. [135].
54	Xe-131m	164 keV 12 d	Solid xenon sample at 90 K compared to gaseous sample at 293 K.	$32\ \pm11$	102	Effect surprisingly large. No details published Cf. [117].
55	Cs-134m	11.2 keV 3 h	$CsJ-CsBr$	—	136	Internal conversion spectrum studied. Differences in relative amounts of discrete energy loss found.
			$CsJ-CsSO_4$	—		

Table 4, continued.

Z	Nuclide	E_0 $T_{1/2}$	Source combination	$\frac{\Delta\lambda}{\lambda}\times 10^3$	Ref.	Comment
1	2	3	4	5	6	7
69	Tm-169m	8.4 keV 4 ns	^{169}Er atoms decaying via negatron emission to ^{169m}Tm implanted into targets of W metal, WO_3, Tm_2O_3, Fe_2O_3, and Al_2O_3.	—	32	Conversion ratios studied. Results: $\alpha_{6s}/\alpha_{5s}=(5.6\pm0.7)\times10^{-2}$ for W metal, $\alpha_{6s}/\alpha_{5s}=(3.0\pm0.6)\times10^{-2}$ for WO_3, $\alpha_{6s}/\alpha_{5s}=(3.5\pm0.6)\times10^{-2}$ for Tm_2O_3, $\alpha_{6s}/\alpha_{5s}=(3\pm1)\times10^{-2}$ for Fe_2O_3, $\alpha_{6s}/\alpha_{5s}=(2\pm2)\times10^{-2}$ for Al_2O_3.
72	Hf-177m	113 keV 0.5 ns	Normal sample compared to sample exposed to electric field of 6×10^6 V/cm.	—	137	Internal conversion electron spectra studied. Line shifts and line shape changes found.
	Hf-179m	161 keV 18.6 s	Hafnium oxide sample compared to metal sample.	13 ± 8	81 82	Effect surprisingly large.
78	Pt-193m	1.64 keV 9.7 ns	^{193}Au atoms decaying via electron capture to ^{193m}Pt incorporated into $AuCl_3$ and Au metal samples.	40 ± 20	138	Effect surprisingly large. Cf. [38].
79	Au-197m	77.3 keV 1.9 ns	Neutral ^{197m}Au atoms compared to ^{197m}Au ions having mean charge of $(+9.5\pm1.5)$.	29 ± 45 -30 ± 60	57 160	Results said to be in agreement with theoretical estimates.
88	Ra-223m$_1$	29.9 keV $T_{1/2}$ unknown	Recoil ions having mean charges between +1 and +12.	—	139 140	Differences in conversion line shapes found.
	Ra-223m$_2$	31.6 keV $T_{1/2}$ unknown	As above.	—	139 140	Dito.
92	U-233m	40 keV $T_{1/2}$ unknown	Normal sample compared to sample exposed to electric field of 6×10^6 V/cm.	—	137	Internal conversion spectra studied. Line shifts and line-shape changes found.
92	U-235m	73 eV 26 min	^{235m}U recoil atoms collected on, and diffused in, bases of platinum, carbon, and silicon to form source pairs:		141 142	
			$U_{metal}-UC_{compound}$	3.18 ± 0.50		
			$U_{metal}-USi_{compound}$	2.21 ± 0.36		
			$USi_{compound}-UC_{compound}$	0.97 ± 0.43		
			^{235m}U recoil atoms collected on copper and platinum, collectors being both in vacuum and argon, and yielding among other combinations the following:		143	Largest decay rate variation ever reported. Value calculated from Table 1 in [143]. Half-life differences found between low-energy and high-energy parts of conversion electron spectrum.
			U in Pt (argon) — U in Cu (vacuum)	133 ± 12		
			^{235m}U recoil atoms collected on Au, Pt, Ni, Cu, and V collectors being both in vacuum and argon and yielding among other source pairs the following:		144	Values calculated from column 4 of Table 1 in [144]. Cf. [147].
			U in Au (vacuum) — U in Pt (vacuum)	18 ± 9		
			U in Au (vacuum) — U in Ni (vacuum)	51 ± 10		
			U in Au (vacuum) — U in Cu (vacuum)	45 ± 14		
			U in Au (vacuum) — U in V (vacuum).	57 ± 12		
			Similar to above using transition metals as collectors the most extreme case being the following source pair:		145	For details of experimental techniques, see [77].
			U in Mn — U in Pd.	52 ± 2		
92			^{235m}U in various oxidation states:		146	Decay constant difference between U_3O_8 and UO_2 samples calculated from Fig. 1 in [146].
			UO_3-UO_2	56 ± 11		
			$U_3O_8-UO_2$.	51 ± 11		

Table 4, continued.

Z	Nuclide	E_0 $T_{1/2}$	Source combination	$\frac{\Delta\lambda}{\lambda}\times 10^3$	Ref.	Comment
1	2	3	4	5	6	7
93	Np-237m	59.5 keV 63 ns	^{237m}Np recoil ions having mean charge of about +14 compared to ions with mean charge smaller than +5.	3 ± 2	56	
94	Pu-239m$_1$	7.85 keV $T_{1/2}$ unknown	Oxide samples compared to hydroxide samples.	—	148	Conversion ratios studied. Results include: $\alpha_{4s\frac{1}{2}}/\alpha_{4p\frac{1}{2}} = (120\pm 7)\times 10^{-2}$, $\alpha_{4s\frac{1}{2}}/\alpha_{4p\frac{3}{2}} = (115\pm 5)\times 10^{-2}$, and $\alpha_{4p\frac{1}{2}}/\alpha_{4p\frac{3}{2}} = (96\pm 4)\times 10^{-2}$ for oxide sample, $\alpha_{4s\frac{1}{2}}/\alpha_{4p\frac{1}{2}} = (142\pm 8)\times 10^{-2}$, $\alpha_{4s\frac{1}{2}}/\alpha_{4p\frac{3}{2}} = (129\pm 5)\times 10^{-2}$, and $\alpha_{4p\frac{1}{2}}/\alpha_{4p\frac{3}{2}} = (92\pm 4)\times 10^{-2}$ for hydroxide sample.
	Pu-239m$_2$	57.2 keV $T_{1/2}$ unknown	Comparison of chloride, hydroxide, and oxide samples exposed to electrostatic field of about 6×10^6 V/cm.	—	149	Internal conversion electron spectra studied. Line shape changes found.

together with results from other new fields such as ESCA, to extend today's knowledge on real chemical bonds.

Many problems, however, call for more extensive work. The theoretical understanding of the problems involved is still comparatively incomplete, and the quantitative interpretation of experimental results therefore often extremely difficult or even impossible. On the other hand, the experimental accuracy achieved so far must be considerably improved to make possible more unambiguous statements. Consequently, the field as a whole is believed to provide challenging tasks to the interested scientist for many years to come.

Acknowledgements

The authors would like to thank Prof. G. Brunner, who initiated the research program on nuclear decay rate variations at the Zentralinstitut für Isotopen- und Strahlenforschung, for many interesting discussions on the subject. Our thanks are also due to Prof. K. Wetzel for his continuing support and various useful hints.

[1] S. DeBenedetti, F. DeS. Barros, and G. R. Hoy, Ann. Rev. Nucl. Sci. **16,** 31 [1966].
[2] G. T. Emery, Ann. Rev. Nucl. Sci. **22,** 165 [1972].
[3] P. Marmier and E. Sheldon, Physics of Particles and Nuclei, Academic Press, New York 1969.
[4] T. Mayer-Kuckuk, Physik der Atomkerne, B. G. Teubner, Stuttgart 1974.
[5] C. Bhalla and M. E. Rose, Phys. Rev. **128,** 1774 [1962].
[6] H. Behrens and J. Jänicke, Numerical Tables for Beta-Decay and Electron Capture, Landolt-Börnstein, New Series, Group I, Volume 3, Springer-Verlag, Berlin 1969.
[7] K. Alder, G. Baur, and U. Raff, Helv. Phys. Acta **44,** 514 [1971].
[8] M. E. Rose, Phys. Rev. **49,** 727 [1936].
[9] L. Durand III, Phys. Rev. **135,** B 310 [1964].
[10] D. H. Wilkinson, Nucl. Phys. **A 150,** 478 [1970].
[11] M. S. Freedman, Ann. Rev. Nucl. Sci. **24,** 209 [1974].
[12] B. Crasemann, Nucl. Instr. Meth. **112,** 33 [1973].
[13] M. L. Perlman, Brookhaven Nat. Lab. Rep. BNL-50100 [1968].
[14] K. Alder, J. Hadermann, and U. Raff, Phys. Lett. **30 A,** 487 [1969].
[15] D. Liberman, J. T. Waber, and D. T. Cromer, Phys. Rev. **A 137,** 27 [1965].
[16] P. Benoist-Gueutal, Ann. Phys. **8,** 593 [1953].
[17] J. N. Bahcall, Phys. Rev. **129,** 2683 [1963].
[18] E. Vatai, Nucl. Phys. **A 156,** 541 [1970].
[19] G. K. Wertheim, Mössbauer Effect: Principles and Applications, Academic Press, New York 1964.
[20] R. L. Mössbauer, Angew. Chem. **14,** 524 [1971].
[21] H. Hofmann-Reinecke, U. Zahn, and H. Daniel, Phys. Lett. **47 B,** 494 [1973].
[22] K. V. Makariunas, Proc. Intern. Conf. Mössbauer Spectroscopy, Vol. I, p. 495 (Cracow, August 25–30, 1975).
[23] S. A. Moszkowski, in: K. Siegbahn (ed.), Alpha-, Beta- and Gamma-Ray Spectroscopy, Vol. II, p. 863, North-Holland Publ. Comp., Amsterdam 1966.
[24] M. A. Listengarten, in: L. A. Sliv (ed.), Gamma-Luchi, p. 271, Akademii Nauk SSSR, Moscow 1961.
[25] N. Tralli and J. Goertzel, Phys. Rev. **83,** 399 [1951].
[26] V. A. Krutov, Izv. Akad. Nauk SSSR, Ser. Fiz. **22,** 162 [1958].
[27] V. A. Krutov and K. Mueller, Izv. Akad. Nauk SSSR, Ser. Fiz. **22,** 171 [1958].

[28] M. E. Rose, Multipole Fields, John Wiley Inc., New York 1955.
[29] V. A. Krutov and V. N. Fomenko, Ann. Physik **21,** 291 [1968].
[30] V. A. Krutov and V. N. Fomenko, Izv. Akad. Nauk SSSR, Ser. Fiz. **33,** 84 [1969].
[31] J.-P. Bocquet, Y. Y. Chu, O. C. Kistner, M. L. Perlman, and G. T. Emery, Phys. Rev. Lett. **17,** 809 [1966].
[32] T. A. Carlson, P. Erman, and K. Fransson, Nucl. Phys. **A 111,** 371 [1968].
[33] K. V. Makariunas, R. A. Kalinauskas, and R. I. Davidonis, Zh. Eksp. Teor. Fiz. **60,** 1569 [1971].
[34] F. Pleiter and B. Kolk, Phys. Lett. **34 B,** 296 [1971].
[35] B. Martin and R. Schulé, Physics Lett. **46 B,** 367 [1973].
[36] I. M. Band, L. A. Sliv, and M. B. Trzhaskovskaya, Nucl. Phys. **A 156,** 170 [1970].
[37] K. Alder, U. Raff, and G. Baur, Helv. Phys. Acta **45,** 771 [1972].
[38] U. Raff, K. Alder, and G. Baur, Helv. Phys. Acta **45,** 428 [1972].
[39] P. Rüegsegger and W. Kündig, Helv. Phys. Acta **46,** 165 [1973].
[40] R. N. Verma and G. T. Emery, Phys. Rev. **B 9,** 3666 [1974].
[41] P. Roggwiller and W. Kündig, Phys. Rev. **B 11,** 4179 [1975].
[42] F. Smend, J. Borchert, and H. Langhoff, Z. Phys. **248,** 326 [1971].
[43] L. M. Dautov, M. M. Kadykenor, and D. K. Kaipov, Proc. Intern. Conf. Mössbauer Spectroscopy, Vol. I, p. 493 (Cracow, August 25–30, 1975).
[44] R. Der and M. Nagel: Ein FORTRAN-Programm zur Berechnung von Koeffizienten der inneren Konversion unter Berücksichtigung der Abschirmung und der endlichen Ausdehnung des Kernes (unpublished report) [1974].
[45] M. Nagel, unpublished report [1973].
[46] K.-P. Dostal, unpublished report [1974].
[47] P. Benoist-Gueutal, C. R. Acad. Sci. Paris **236,** 691 [1953].
[48] P. Benoist-Gueutal, J. Phys. Rad. **16,** 595 [1955].
[49] V. A. Erma, Phys. Rev. **105,** 1784 [1957].
[50] T. A. Carlson, C. C. Lu, T. C. Tucker, C. W. Nestor, and F. B. Malik, Oak Ridge Nat. Lab. Rep. ORNL-4614 [1970].
[51] W. Rubinson and M. L. Perlman, Phys. Lett. **40 B,** 352 [1972].
[52] K. Alder, G. Baur, and U. Raff, Phys. Lett. **34 A,** 163 [1971].
[53] C. A. Accardo, Phys. Rev. Lett. **1,** 180 [1958].
[54] V. J. Ilyushchenko, E. D. Donets, and V. A. Alpert, Dubna Joint Inst. Nucl. Res. Prep. P7-4688 [1969].
[55] V. J. Goldansky and V. S. Letokhov, Zh. Eksp. Teor. Fiz. **67,** 513 [1974].
[56] R. J. Walen, M. Valadres, and C. Briançon, J. Phys. **32,** C4-145 [1971].
[57] M. Ulrickson, R. Hensler, D. Gordon, N. Benezer-Koller, and H. DeWaard, Phys. Rev. **C 9,** 326 [1974].
[58] R. W. Dixon and N. Bloembergen, J. Chem. Phys. **41,** 1739 [1964].
[59] H. Leuenberger, Inauguraldissertation, Basel 1971.
[60] St. Gagneux, P. Huber, H. Leuenberger, and P. Nyikos, Helv. Phys. Acta **43,** 39 [1970].
[61] M. Nishi and S. Shimizu, Phys. Rev. **B 5,** 3218 [1972].
[62] P. Auric and J. I. Vargas, Chem. Phys. Lett. **27,** 229 [1974].
[63] P. Huber and H. H. Staub, Atomphysik, Ernst Reinhardt Verlag AG, Basel 1976.
[64] R. A. Porter and W. G. McMillan, Phys. Rev. **117,** 795 [1960].
[65] H. Mazaki, T. Nagatomo, and S. Shimizu, Phys. Rev. **C 5,** 1718 [1972].
[66] W. K. Hensley, W. A. Basset, and J. R. Huizenga, Science **181,** 1164 [1973].
[67] T. Mukoyama and S. Shimizu, Phys. Lett. **50 A,** 258 [1974].
[68] H. G. Drickamer and C. W. Frank, Ann. Rev. Phys. Chem. **23,** 39 [1972].
[69] D. H. Byers and R. Stump, Phys. Rev. **112,** 77 [1958].
[70] J. A. Cooper, Univ. Calif. Rep. UCRL-16910 [1966].
[71] A. Olin and K. T. Bainbridge, Phys. Rev. **179,** 450 [1969].
[72] P. Rüegsegger, Inauguraldissertation, Zürich 1972.
[73] J. A. Cooper, J. M. Hollander, and J. O. Rasmussen, Phys. Rev. Lett. **15,** 680 [1965].
[74] K. T. Bainbridge, M. Goldhaber, and E. Wilson, Phys. Rev. **90,** 430 [1953].
[75] G. Harbottle, C. Koehler, and R. Withnell, Rev. Sci. Instr. **44,** 55 [1973].
[76] K.-P. Dostal and E. D. Pabst, Nucl. Instr. Meth. **135,** 99 [1976].
[77] M. Nève de Mévergnies, Nucl. Instr. Meth. **109,** 145 [1973].
[78] R. D. Evans, The Atomic Nucleus, McGraw-Hill Book Comp., New York 1955.
[79] P. Huber, St. Gagneux, and H. Leuenberger, Phys. Lett. **27 B,** 86 [1968].
[80] P. Nyikos, St. Gagneux, P. Huber, H. R. Kobel, and H. Leuenberger, Helv. Phys. Acta **43,** 412 [1970].
[81] R. Beeler, L. Balsenc, and J. Laplace, J. Radioanal. Chem. **10,** 257 [1972].
[82] R. Beeler, L. Balsenc, and J. Laplace, Paper presented at the Conférence internationale sur les tendances modernes de l'analyse par activation (Sacclay, October 2–6, 1972).
[83] J. Eugster, Phys. Blätter **23,** 267 [1967].
[84] E. Segrè and C. E. Wiegand, Phys. Rev. **81,** 284 [1951].
[85] J. J. Kraushaar, E. D. Wilson, and K. T. Bainbridge, Phys. Rev. **90,** 610 [1953].
[86] R. F. Leininger, E. Segrè, and C. E. Wiegand, Phys. Rev. **81,** 280 [1951].
[87] H. W. Johlige, D. C. Aumann, and H.-J. Born, Phys. Rev. C **2,** 1616 [1970].
[88] R. Bouchez, J. Tobailem, J. Robert, R. Muxart, R. Mellet, R. Daudel, and P. Daudel, J. Phys. Rad. **17,** 363 [1956].
[89] K. T. Bainbridge and E. Baker, Bull. Am. Phys. Soc. **4,** 278 [1959].
[90] W. B. Gogarty, S. S. Kistler, and E. B. Christiansen, Off. Naval Res. Technical Rep. No. VII [1963].
[91] R. Daudel, Rev. Sci. **85,** 162 [1947].
[92] E. Segrè, Phys, Rev. **71,** 274 [1947].
[93] R. Bouchez, R. Daudel, P. Daudel, and R. Muxart, J. Phys. Rad. **8,** 336 [1947].
[94] R. Bouchez, P. Daudel, R. Daudel, and R. Muxart, C. R. Acad. Sci. **227,** 525 [1948].
[95] R. Bouchez, P. Daudel, R. Daudel, R. Muxart, and A. Rogozinski, J. Phys. Rad. **10,** 201 [1949].
[96] P. Benoist, R. Bouchez, P. Daudel, R. Daudel, and A. Rogozinski, Phys. Rev. **76,** 1000 [1949].
[97] E. Segrè and C. E. Wiegand, Phys. Rev. **75,** 39 [1949].
[98] R. F. Leininger, E. Segrè, and C. E. Wiegand, Phys. Rev. **76,** 897 [1949].
[99] P. Benoist-Gueutal, Physica **18,** 1192 [1952].
[100] P. Kemény, Rev. Roum. Phys. **13,** 901 [1968].
[101] P. Auric and J. I. Vargas, Chem. Phys. Lett. **15,** 366 [1972].

[102] P. Kemény, Magyar Fiz. Folyoir. **19,** 483 [1971].
[103] H. Leuenberger, Physica **64,** 621 [1973].
[104] W. Kündig, to be published in: Proc. Intern. Conf. Mössbauer Spectroscopy, Vol. II (Cracow, August 25—30, 1975).
[105] P. Kemény, Radiochem. Radioanal. Lett. **2,** 119 [1969].
[106] S. Chakraborty, Paper presented at the Session d' Automne de la Société Suisse de Physique (Luzern, October 13—14, 1972).
[107] P. G. Bergamini, G. Palmas, F. Piantelli, and M. Rigato, Phys. Rev. Lett. **18,** 468 [1967].
[108] P. Kemény, Rev. Roum. Phys. **13,** 485 [1968].
[109] G. J. Gleason and S. A. Reynolds, Oak Ridge Nat. Lab. Rep. ORNL-TM-2876 [1970].
[110] W. H. Zoller, P. K. Hopke, J. L. Fasching, E. S. Macias, and W. B. Walters, Phys. Rev. **C 3,** 1699 [1971].
[111] P. Nyikos, Inauguraldissertation, Basel 1972.
[112] P. Nyikos, H. P. Bier, P. Huberit, H. R. Kobel, H. Leuenberger, and H. G. Seiler, Helv. Phys. Acta **46,** 444 [1973].
[113] P. M. Sherk, Phys. Rev. **75,** 789 [1949]
[114] K.-E. Bergkvist, Physica Scripta **4,** 23 [1971].
[115] K. Junker, Acta Phys. Austr. **34,** 117 [1971].
[116] S. Chakraborty, Helv. Phys. Acta **46,** 53 [1973].
[117] P. Kemény, Radiochem. Radioanal. Lett. **2,** 41 [1969].
[118] F. T. Porter and M. S. Freedman, Phys. Rev. **C 3,** 2285 [1971].
[119] M. Fujioka and K. Hisatake, Phys. Lett. **B 40,** 99 [1972].
[120] R. Beeler, L. Balsenc, and J. Laplace, Helv. Phys. Acta **45,** 929 [1972].
[121] F. T. Porter, M. S. Freedman, and F. Wagner, Jr., Phys. Rev. **C 3,** 2246 [1971].
[122] P. Rüegsegger and W. Kündig, Helv. Phys. Acta **45,** 897 [1972].
[123] P. Rüegsegger and W. Kündig, Phys. Lett. **39 B,** 620 [1972].
[124] W. Weihrauch, W.-D. Schmidt-Ott, F. Smend, and A. Flammersfeld, Z. Phys. **209,** 289 [1968].
[125] A. Olin, Phys. Rev. **C 1,** 1114 [1970].
[126] K. T. Bainbridge, M. Goldhaber, and E. Wilson, Phys. Rev. **84,** 1260 [1951].
[127] K. T. Bainbridge, Chem. Eng. News **30,** 654 [1952].
[128] H. Leuenberger, St. Gagneux, P. Huber, H. R. Kobel, P. Nyikos, and H. Seiler, Helv. Phys. Acta **43,** 411 [1970].
[129] H. Leuenberger, P. Huber, P. Nyikos, H. R. Kobel, and H. Seiler, Helv. Chim. Acta **55,** 961 [1972].
[130] T. Hamada, Technical Summary Report for the 11th Japan Conference on Radioisotopes, p. 149 (Tokyo, November 13—15, 1973).
[131] H. Mazaki, Butsuri **26,** 504 [1971].
[132] J. P. Bocquet, Y. Y. Chu, G. T. Emery, and M. L. Perlman, Phys. Rev. **167,** 1117 [1968].
[133] G. T. Emery and M. L. Perlman, Phys. Rev. **B 1,** 3885 [1970].
[134] A. C. Malliaris and K. T. Bainbridge, Phys. Rev. **149,** 958 [1966].
[135] R. Schulé, Dissertation, Heidelberg 1973.
[136] B. Martin and R. Schulé, Proc. Intern. Conf. Inner Shell Ionization Phenomena, p. 1834 (Atlanta/USA, 1972).
[137] T. Novakov and J. M. Hollander, Phys. Lett. **13,** 301 [1964].
[138] A. Marelius, Ark. Fys. **37,** 427 [1968].
[139] M. Valadres, R. J. Walen, and C. Briançon, C. R. Acad. Sci. **B 263,** 213 [1966].
[140] W. Gelletly, J. S. Geiger, and J. S. Merritt, Can. J. Phys. **48,** 993 [1970].
[141] S. Shimizu and H. Mazaki, Phys. Lett. **17,** 275 [1965].
[142] H. Mazaki and S. Shimizu, Phys. Rev. **148,** 1161 [1966].
[143] M. Nève de Mévergnies, Phys. Lett. **26 B,** 615 [1968].
[144] M. Nève de Mévergnies, Phys. Rev. Lett. **23,** 422 [1969].
[145] M. Nève de Mévergnies, Phys. Rev. Lett. **29,** 1188 [1972].
[146] M. Nève de Mévergnies and P. Del Marmol, Phys. Lett. **49 B,** 428 [1974].
[147] M. Nève de Mévergnies, Vacuum **22,** 463 [1972].
[148] T. Novakov, R. Stepić, and P. Janičijević, Fizika, Suppl. **1,** 53 [1969].
[149] T. Novakov and J. M. Hollander, Phys. Rev. Lett. **21,** 1133 [1968].
[150] H. C. Pauli and U. Raff, Comp. Phys. Comm. **9,** 392 [1975].
[151] E. Vatai and C. Ujhelyi, Proc. Intern. Conf. Inner Shell Ionisation Phenomena (1972).
[152] J. F. Emery, S. A. Reynolds, E. I. Wyatt, and G. I. Gleason, Nucl. Sci. Eng. **48,** 319 [1972].
[153] I. Dema and G. Harbottle, VII. Intern. Hot Atom Chem. Sympos. (Jülich, 1973).
[154] B. Jenschke, Spring Conf. Ger. Phys. Soc. (1974).
[155] J. A. Johnson, I. Dema, and G. Harbottle, Radichim. Act.
[156] R. Beeler, R. Balsenc, and J. Laplace, J. Radioanal. Chem. **15,** 489 [1973].
[157] W. K. Sinclair and A. F. Holloway, Nature **167,** 365 [1951].
[158] J. I. Kim, F. Buheitel, and H.-J. Born, Radiochim. Act. **22,** 153 [1975].
[159] J. S. Geiger, R. L. Graham, and M. W. Johns, Can. Journ. phys. **47,** 949 [1969].
[160] L. E. Young, R. Brenn, and G. D. Sprouse, Bull. Amer. Phys. Soc. **18,** 655 [1973].